Australian Earthquake Engineering Society
2022 National Conference, 24-25 November 2022
Mount Macedon, Victoria, Australia

Observations from the 2022 Arthur River, Western Australia, Earthquake Swarm

Ruth Murdie[1], Robert Pickle[2], Huaiyu Yuan[3], David Love[4], Vic Dent[5], Meghan S. Miller[1], Justin Whitney[6]

1. *Geological Survey of Western Australia; Ruth.Murdie@dmirs.wa.gov.au*
2. *Australian National University; Robert.Pickle@anu.edu.au*
3. *Geological Survey of Western Australia; Huiayu.Yuan@dmirs.wa.gov.au*
4. *Seismological Association of Australia; david@earthquake.net.au*
5. *vic_dent@yahoo.com*
6. *Department of Fire and Emergency Services; Justin.Whitney@dfes.wa.gov.au*

Abstract

On 5th January 2022, a M_{La} 4.0 earthquake in Western Australia's Southern Wheatbelt triggered a major sequence of events. Geoscience Australia (GA) initially located this event 20 km north-east of Arthur River. However, these measurements relied only on data from the Australian National Seismograph Network (ANSN), the ANU Seismometers in Schools network, and the US Geological Survey's Global Seismic Network (IU) with the nearest station ~50 km from the epicentre.

A local network was deployed to complement data from an existing temporary array in the Yilgarn Craton and the ANSN. Data from all stations were passed through a machine-learning detection algorithm which had been trained to identify phase arrivals of very small earthquakes with high precision. Using double-difference techniques, the relocated hypocentres cannot be associated with a clear planar fault surface. Rather, the hypocentres appear to form a "rupture volume" that may represent a 3-dimensional region of deformation, which appears to be controlled by pre-existing geological structure. This observation is similar to other high-resolution records of aftershock sequences in Australia. The future objective now is to characterise the earthquake sources, investigate the local stress field and assess ground-motion attenuation characteristics in the region.

Keywords: southwest seismic zone, swarm, machine learning, InSAR.

1 Background

The South West Seismic Zone as coined by Doyle (1971), is one of the most seismically active areas of the Australian continent with consistent low-magnitude seismicity. The region has also hosted five of nine of Australia's known surface rupturing earthquakes over a five-decade period (Clark *et al.*, 2020), including: Meckering M_W 6.5 in 1968; Cadoux M_L 6.1; and Lake Muir

M_W 5.3 2018. However, low-magnitude events (M_{La} < 3.0) are a frequent occurrence here, often occurring in clusters and swarms (e.g., Leonard, 2002; Dent, 2009; 2015).

On 5th January 2022, Western Australia's Southern Wheatbelt experienced a magnitude M_{La} 4.0 earthquake triggering a swarm of events which continued for over six months. This was to be the first of three major shocks in a swarm of smaller events. The largest event in the sequence (M_{La} 4.8, in agreement with GA's estimate) occurred on 24th January. This event was felt across the Wheatbelt region and into the Perth metropolitan area. Another large (M_{La} 4.3) event occurred on 1st February. While earthquake swarms are common in the region, it was the first swarm known to have occurred in the Arthur River region. Geoscience Australia (GA) located the initial event approximately 20 km north-east of Arthur River at a depth of 7 km (https://earthquakes.ga.gov.au/event/ga2022aigaei). However, these measurements relied only on data from the Australian National Seismograph Network (ANSN), the Seismometers in Schools (SIS; Balfour *et al.*, 2014; Salmon *et al.*, 2022) stations run by Australian National University (ANU), and the US Geological Survey's Global Seismic Network (IU) with the nearest station being approximately 50 km away. Depths of earthquakes in the southwest seismic zone have always been uncertain given the sparseness of monitoring networks.

An ARC Linkage Project, "Enhanced 3-D Seismic Structure of Southwest Australia" (SWAN), led by ANU with collaboration from GA, Macquarie University, the Geological Survey of Western Australia (GSWA) and the Department of Fire and Emergency Services (DFES) has an objective to create a suite of 3-D models of the crust and lithosphere and record local seismicity to better locate the frequent events. SWAN had 27 seismometers (Murdie *et al.*, 2020) deployed around southwest WA, three of which were closer than any of the ANSN stations. However, these were still ~20 km away from the swarm. Due to border closures and travel restrictions during the pandemic, GA were not able to deploy Rapid Deployment Kits (RDKs), but GSWA and the University of Western Australia were able to deploy 10 additional seismometers near the initial event.

Six sites were occupied by five 5 s SmartSolo seismometers, and three very short-term sites were occupied courtesy of Alby Judge and Vic Dent. The aim of the rapid deployment was twofold: to determine the depth of the events which required a site within close proximity to the swarm, and; to record near-source ground-motion data from any subsequent moderate-to-large magnitude aftershocks. Sites SWNNA and SWNNB were supplemented with accelerometers (RefTek 147A). A list of locations and occupation dates can be found in Table 1 and in Figure 1.

Table 1. Locations and running times of stations of the RDKs at Arthur River.

Station	Code	Lat	Long	AHD	installed	removed	instrument
Puntapin	SWNNA	-33.3261	117.4019	220	10/01/2022	04/04/2022	smartsolo 5s
Warup	SWNNB	-33.3629	117.1909	294	10/01/2022	06/05/2022	smartsolo 5s
Piesseville	SWNNC	-33.1939	117.2890	250	10/01/2022	04/04/2022	smartsolo 5s
East Arthur	SWNND	-33.4191	117.0395	231	10/01/2022	running	smartsolo 5s
Arthur River	SWNNE	-33.2844	117.0303	240	10/01/2022	running	smartsolo 5s
Mialling	SWNNF	-33.3439	116.9502	210	10/01/2022	running	smartsolo 5s
Mialling	SWNNF	-33.3439	116.9502	210	07/02/2022	running	reftek 147A
Clifton Park	SWNNG	-33.4182	117.0078		07/02/2022	running	smartsolo 5s
Clifton Park	SWNNG	-33.4182	117.0078		07/02/2022	running	reftek 147A
Tuchbrook	SWNNH	-33.3882	116.8996	328	07/02/2022	running	smartsolo 5s
Alby1	AJ01	-33.3568	116.9742				
Alby2	AJ02	-33.3472	117.0029				
Ably3	AJ03	-33.3768	116.9928				
AJ1c	SWNNI	-33.3499	116.9688	216	6/05/2022	running	smartsolo 5s
Burgess	SWNNJ	-33.3657	116.9908	551	6/05/2022	running	smartsolo 5s
Burgess	SWNNJ	-33.3657	116.9908	551	6/05/2022	running	reftek 147A
New site	SWNNK	-33.381	116.972		18/06/2022	running	smartsolo 5s

The depth of earthquakes in the SWSZ as reported by the ANSN, have large errors due to the sparsity of the ANSN stations. However, large surface waves that are commonly observed in seismic signals from earthquakes in this region (Allen *et al.*, 2006; Somerville *et al.*, 2009; Allen, 2020), together with the propensity for moderate-sized earthquakes to cause surface deformation (Dawson *et al.*, 2008; Clark *et al.*, 2020), suggest predominantly shallow hypocentres. It has been an objective of seismologists in WA to better determine these depths in order to further understand their origin.

Data from the short-term RDKs were set to record at 250 samples per second and were downloaded every three weeks to three months once solar infrastructure was connected. Data were also collected from the closest three SWAN stations.

Waveforms recorded on the SmartSolo nodes for the 24th January M_{La} 4.8 event showed clear *P*, *S* and surface wave arrivals (Figure 2). The short time gaps between the *P* and *S* arrivals and the surface waves suggests that this event possessed a shallow hypocentre. The nearest two sites saturated for the main event.

Figure 1: Locations of the stations used in the study from the ANSN (black squares), SIS (black triangles), SWAN (green circles) and Arthur River RDK stations (pink circles).

2 InSAR Observations

The Interferometric Synthetic Aperture Radar (InSAR) coseismic displacement interferogram from Sentinel-1 LOS on both the ascending track and descending track showed an uplift of approximately 2 cm in the vicinity of the epicentres of the swarm after the M_{La} 4.8 shock (Figure 3). The location of the surface deformation was ~11 km SW of Geoscience Australia's preferred location based on ANSN data.

The InSAR data suggested that the rupture surface was very shallow but had not breached the surface and was on a NE-SW reverse fault possibly dipping to the northwest. No evidence of surface rupture was identified during any seismic deploys nor have any been reported by local landowners. Surface deformation was limited to some cracking in the fields, a new water seep, toppled stones from a nearby dam. Some local masonry buildings near the observed surface deformation also suffered minor cracking.

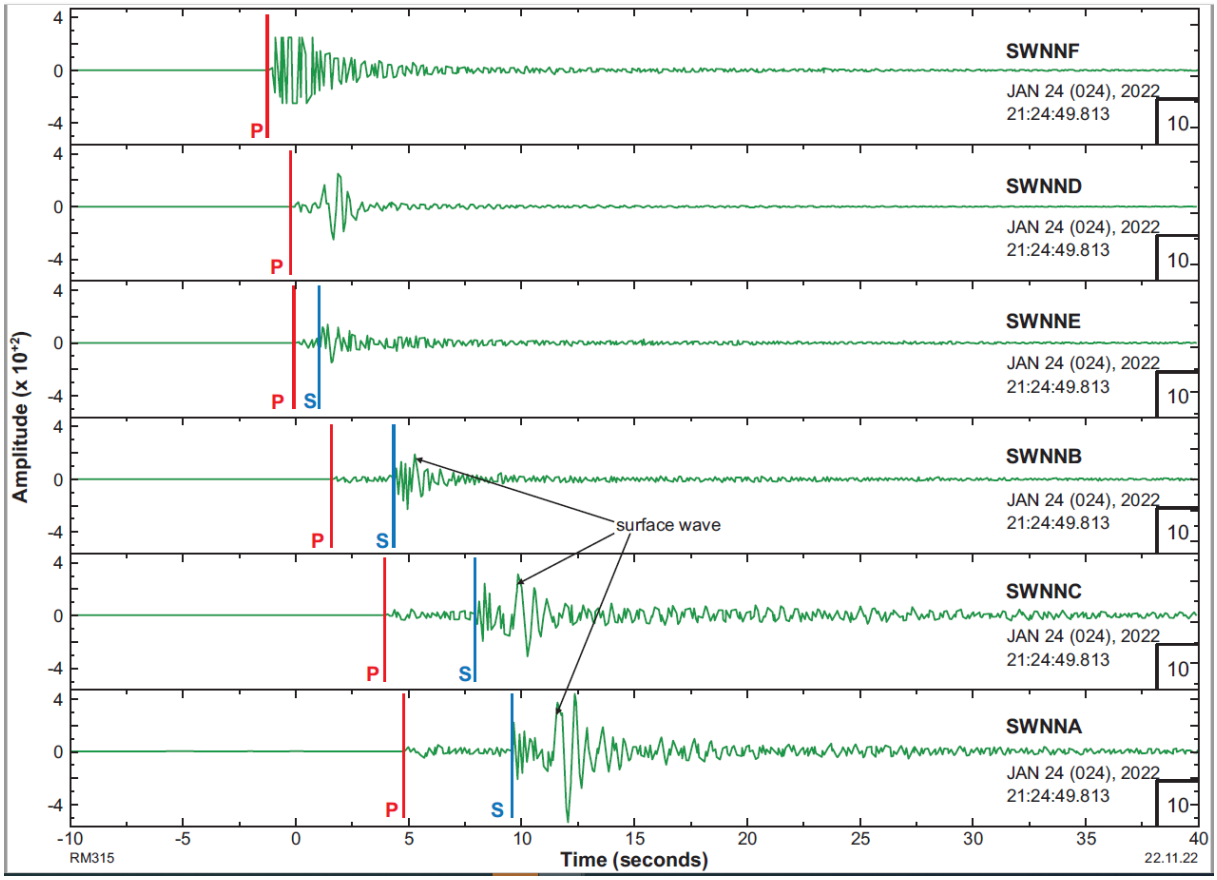

Figure 2: Screen grab from a "quick plot" from the SAC software of the seismograms of the 24th January M_{La} 4.8 event as recorded on the SmartSolo instruments.

3 Machine Learning

Data was ingested into a customised machine-learning detection algorithm based on EQTransformer (Mousavi *et al.*, 2020) and trained with a global dataset of over one million *P* and *S* arrivals from 450 thousand globally distributed local (< 350km) events (STEAD; Mousavi *et al.*, 2019). These picks were from a variety of tectonic settings and 70% are classified as being manually reviewed. These picks were then associated to events using the REAL algorithm (Zhang *et al.*, 2019) and relocated in 3D using NonLinLoc (Lomax *et al.*, 2000) and the AuSREM 3D velocity model (Kennett and Salmon, 2012; Salmon *et al.*, 2013). Finally, event hypocentres were adjusted via a double-differencing algorithm based on (Waldhauser and Ellsworth, 2000).

Events in the catalogue have a mean RMS error of 0.26 seconds and mean horizontal and depth uncertainties of 3.5 and 4.4 km respectively. On average 7.5 *P* and 8.0 *S* phase picks from stations nearer than 2.0 degrees were used to locate each event.

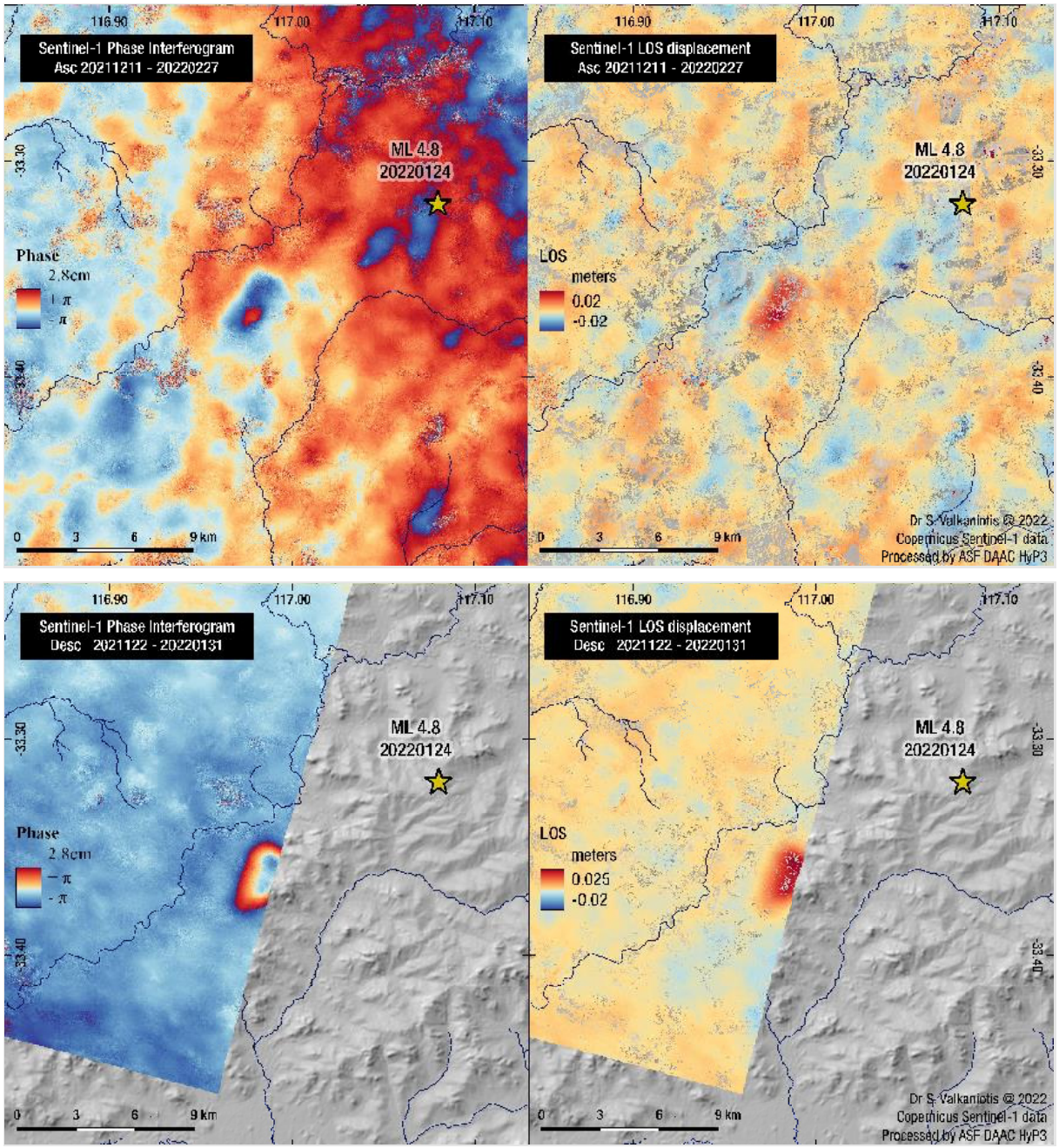

Figure 3 a) Sentinel-1 ascending track coseismic interferogram over the M_{La} 4.8 main shock region which is strongly affected by noise. b) Sentinel-1 descending track coseismic interferogram over the same area which clearly shows the surface expression of the event. Note that in each case the epicentre of the event is at the location published by GA using only the permanent ANSN stations. Source: Sotiris Valkaniotis.

4 Swarm Locations

Comparison of the GA locations and our machine-learning-based locations show a much tighter clustering of events (Figure 4). Additionally, the higher-precision locations shifted initial depth estimates from 15-20 km to 0-5 km and reduced hypocentre uncertainty in all orientations by a factor of 2 or more. The updated epicentral locations are also now more consistent with the highest shaking intensities reported through GA's felt report system (e.g., Allen *et al.*, 2019) and coincide with greatest ground displacement observed through the InSAR analysis.

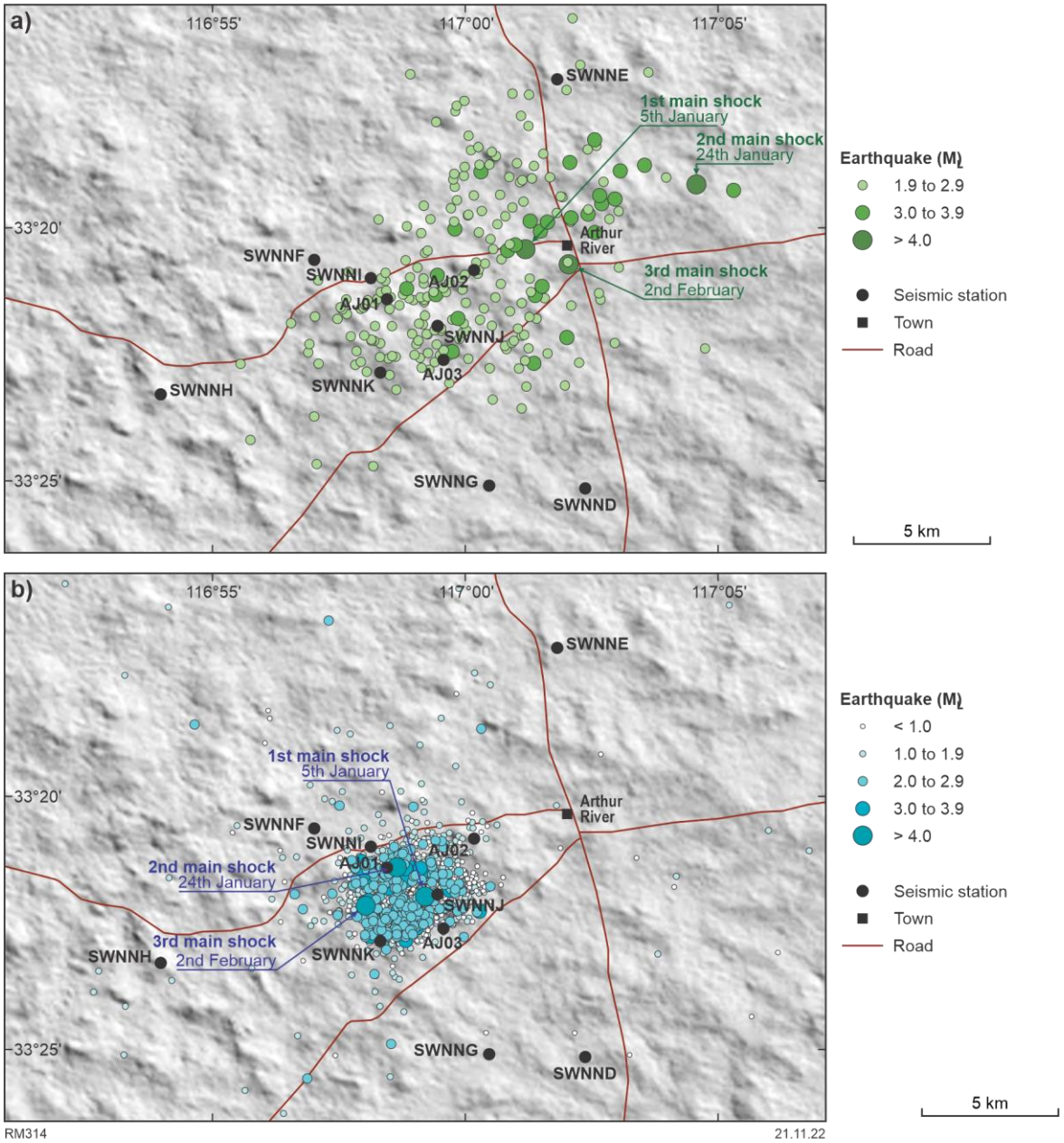

Figure 4a) Earthquake locations as determined by GA using only the ANSN and SIS stations b) Earthquake locations as determined by using the ANSN, SIS, SWAN and RDK stations from 10th to 27th June 2022.

Over the first six months, seven times as many events were recorded by the combined SWAN and RDK networks (1800+) relative to the GA (242) website published between 5th January and 27th June 2022. Many of these events (~1500) were M_{La} < 2.0 which is the general minimum for GA reporting. For events with M_{La} ≥ 2.0, the SWAN and RDK networks only recorded 10 more events than listed in the GA catalogue. By contrast, this may be because GA estimated magnitudes less than M_{La} 2.0 and are thus not available through the online search. Events as small as M_{La} 0.2 were recorded by the RDK network. The depth of most events are less than 7 km.

Figure 5 shows the cumulative number of events plotted against time. This clearly shows a temporary increase in the rate of the swarm activity around the time of the M_{La} 4.8 mainshock, which slowly decays over the ensuing months. Each of the main-shock-events feature a tail of smaller aftershocks. The number of aftershocks has reduced since June 2022, but M_{La} 3.0 events were still occurring in September 2022.

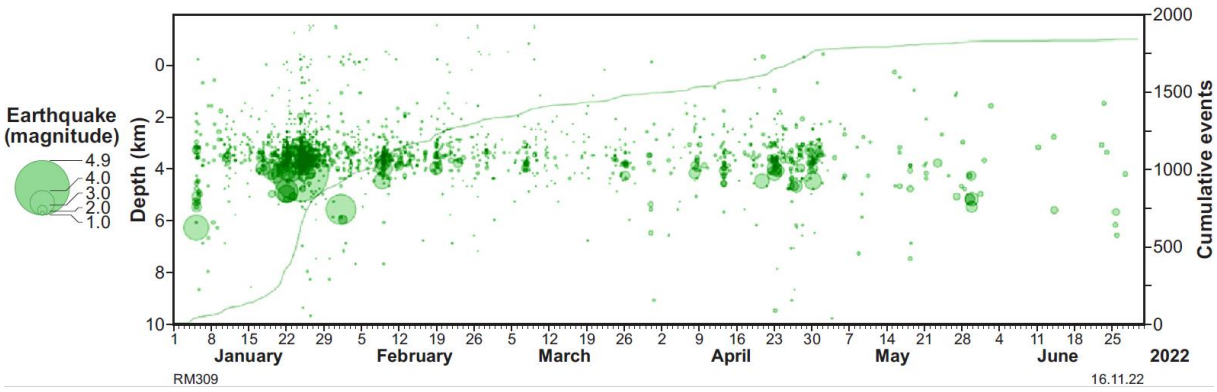

Figure 5: Cumulative number of events with time in the 2022 Arthur River swarm. Individual events are plotted by hypocentral depth and sized by magnitude (see red circles as legend).

5 Comparison with Mapped Geology

The geology of the area consists of Archean granite of the Yilgarn Craton. All the epicentres fall within the same mapped block of monzogranite (Figure 6a, Quentin de Gromard *et al.*, 2021). Plotting the earthquake locations on a map of the total magnetic intensity (TMI; Brett, 2020; Figure 6b), the strong features that show in the area are the east-west trending features of the Widgiemooltha dyke swarm, and the northwest-southeast trending dykes of the Boyagin Dolerite dyke swarm (Figure 6a). Faults in this area tend to manifest as breaks in the magnetic trends where demagnetisation has occurred. In a recent interpretation of the geology by (Quentin de Gromard *et al.*, 2021) there are various faults in the area, one in particular which trends northeast-southwest, tracks right through the centre of the cluster of events. This correlates well with the interpretation from the InSAR images. Analysis of other surface-rupturing earthquakes in Australia indicates that the rupture length and geometry is often controlled by pre-existing geological structure within the host basement rocks (Clark *et al.*, 2020; Yang *et al.*, 2021).

The relocated hypocentres cannot be associated with a clear planar fault surface. Rather, the hypocentres appear to form a “rupture volume” that may represent a 3-dimensional region of deformation, which may be controlled by pre-existing structure. This observation is similar to other high-resolution records of aftershock sequences in Australia, in which the aftershocks do not clearly define a planar rupture plane (e.g., Clark *et al.*, 2020; Brenn *et al.*, 2021).

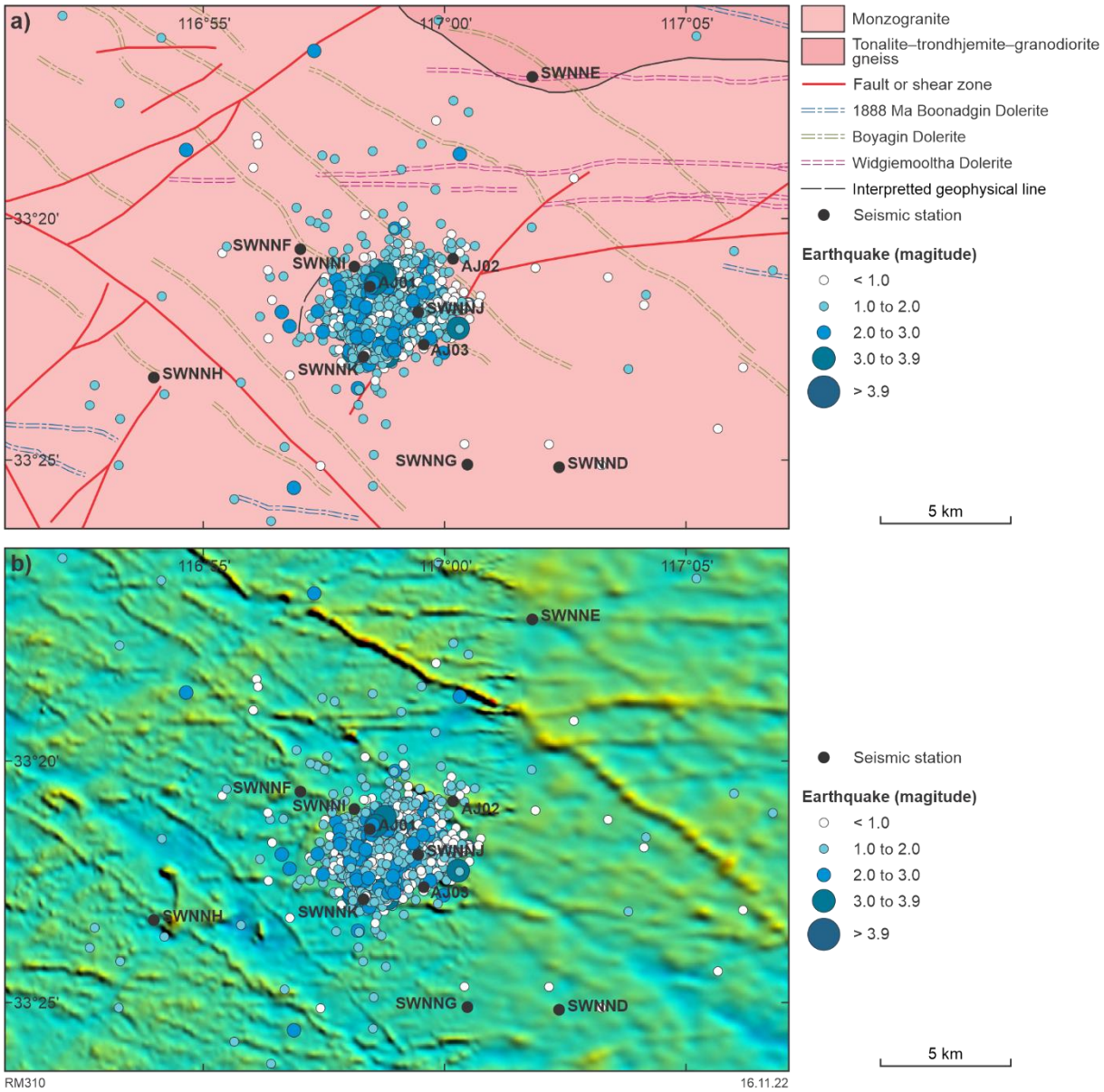

Figure 6: a) Geological map of the area showing the uniform coverage of monzogranite. Dykes and mapped faults are shown. b) The total magnetic intensity image (TMI) of the same area.

6 Conclusion

The 2022 Arthur River, WA, earthquake sequence has presented a unique opportunity to study an earthquake swarm in unprecedented detail. At the time of this earthquake sequence, a network of 27 seismographs were operating in the southwestern region of Western Australia through the SWAN project (Murdie *et al.*, 2020). Following the 5 January M_{La} 4.0 earthquake, RDKs were deployed to the region. Together with the existing stations, these RDKs recorded two further moderate-magnitude earthquakes, including the 24 January M_{La} 4.8 mainshock. These data will offer a number of benefits to seismic hazard modellers, particularly in regard to the high-quality near-source ground motions recorded from the largest events.

Machine learning techniques have been applied to the Arthur River swarm data. Over 1800 earthquakes have been located using these techniques. Data demonstrate shallow hypocentres for these events, with events co-located with satellite-based ground deformation estimates of coseismic surface deformation (Figure 3). The relocated hypocentres cannot be associated with a clear planar fault surface. Rather, the hypocentres appear to form a “rupture

volume" that may represent a 3-dimensional region of deformation, which appears to be controlled by pre-existing structure. This observation is similar to other high-resolution records of aftershock sequences in Australia, in which the aftershocks do not clearly define a planar rupture plane (e.g., Clark *et al.*, 2020; Brenn *et al.*, 2021).

Finally, the data recorded from these temporary networks will be used to improve 3D velocity models and will contribute to an improved understanding of ground-motion attenuation in the Yilgarn Craton. Effects of how seismic energy propagates into and through the Perth Basin will also be assessed.

7 Acknowledgements

The waveforms and preliminary results were collected as part of the Australian Research Council (ARC) funded "Enhanced 3-D Seismic structure for Southwest Australia' Discovery Project LP180101118. The project uses 27 ANSIR (Australian National Seismic Imaging Resource) facility https://www.auscope.org.au/ansir broadband seismometers and data recorders from the pool of instrumentation. Data will be available from AusPass (auspass.edu.au): Australian Passive Seismic Server for network 2P in 2025 following the 2-year data embargo (doi: 10.7914/SN/2P_2020; https://www.fdsn.org/networks/detail/2P_2020/). Additional data are from the Australian National Seismograph Network (AU) network (doi.org/10.26186/144675); Australian Seismometers in Schools network (S1) doi.org/10.7914/SN/S1; and the Global Seismograph Network (IU) station NWAO, doi.org/10.7914/SN/IU). Ruth Murdie publishes with permission of the Executive Director of the Geological Survey of Western Australia.

8 References

Allen, T., A. Carapetis, J. Bathgate, H. Ghasemi, T. Pejić, and A. Moseley (2019). Real-time community internet intensity maps and ShakeMaps for Australian earthquakes, *Australian Earthquake Engineering Society 2019 Conference*, Newcastle, New South Wales.

Allen, T. I. (2020). Seismic hazard estimation in stable continental regions: does PSHA meet the needs for modern engineering design in Australia?, *Bull. New Zeal. Soc. Earthq. Eng.* **53,** 22-36, doi: 10.5459/bnzsee.53.1.22-36.

Allen, T. I., T. Dhu, P. R. Cummins, and J. F. Schneider (2006). Empirical attenuation of ground-motion spectral amplitudes in southwestern Western Australia, *Bull. Seismol. Soc. Am.* **96,** 572–585, doi: 10.1785/0120040238.

Balfour, N. J., M. Salmon, and M. Sambridge (2014). The Australian Seismometers in Schools Network: education, outreach, research, and monitoring, *Seismol. Res. Lett.* **85,** 1063-1068, doi: 10.1785/0220140025.

Brenn, G., S. Shamsalsadati, C. Sippl, and M. Comoglu (2021). Automated relocation of the Petermann Ranges aftershock sequence, *Australian Earthquake Engineering Society 2021 Virtual Conference*.

Brett, J. W. (2020). 40 m magnetic merged grid of Western Australia 2020 version 1, *Geological Survey of Western Australia*pp, www.dmp.wa.gov.au/geophysics.

Clark, D. J., S. Brennand, G. Brenn, M. C. Garthwaite, J. Dimech, T. I. Allen, and S. Standen (2020). Surface deformation relating to the 2018 Lake Muir earthquake sequence, southwest Western Australia: new insight into stable continental region earthquakes, *Solid Earth* **11,** 691–717, doi: 10.5194/se-11-691-2020.

Dawson, J., P. Cummins, P. Tregoning, and M. Leonard (2008). Shallow intraplate earthquakes in Western Australia observed by Interferometric Synthetic Aperture Radar, *J. Geophys. Res.* **113,** B11408, doi: 10.1029/2008JB005807.

Dent, V. (2015). Clustered seismicity in the Southwest Australia Seismic Zone, 2014-2015, *10th Pacific Conference on Earthquake Engineering*, Sydney, New South Wales.

Dent, V. F. (2009). The Beacon, WA earthquake swarm commencing January 2009, *Australian Earthquake Engineering Society 2009 Conference*, Newcastle, New South Wales.

Doyle, H. (1971). Australian seismicity, *Nat. Phys. Sci.* **234,** 174–175, doi: 10.1038/physci234174a0.

Kennett, B. L. N., and M. L. Salmon (2012). AuSREM: Australian seismological reference model, *Aust. J. Earth Sci.* **58,** 1091-1103, doi: 10.1080/08120099.2012.736406.

Leonard, M. (2002). The Burakin WA earthquake sequence Sept 2000 - June 2002, *Austrailain Earthquake Engineering Society 2002 Conference*, Adelaide, South Australia.

Lomax, A., J. Virieux, P. Volant, and C. Berge-Thierry (2000). Probabilistic earthquake location in 3D and layered models; *In* H., T. C., and N., R., Eds., *Advances in seismic event location, Modern approaches in geophysics*. Dordrecht, Springer. **18**.

Mousavi, S. M., W. L. Ellsworth, W. Zhu, L. Y. Chuang, and G. C. Beroza (2020). Earthquake transformer—an attentive deep-learning model for simultaneous earthquake detection and phase picking, *Nat. Commun.* **11,** 3952, doi: 10.1038/s41467-020-17591-w.

Mousavi, S. M., Y. Sheng, W. Zhu, and G. C. Beroza (2019). STanford EArthquake Dataset (STEAD): A Global Data Set of Seismic Signals for AI, *IEEE Access*, doi: 10.1109/ACCESS.2019.2947848.

Murdie, R., K. Gessner, M. Miller, M. Salmon, H. Yuan, J. Whitney, S. Gray, and T. Allen (2020). Geological Survey of Western Australia: SWAN takes off - a new seismic monitoring project in Western Australia, *Preview* **208,** 28-29, doi: 10.1080/14432471.2020.1828423.

Quentin de Gromard, R., T. J. Ivanic, and I. Zibra (2021). Pre-Mesozoic interpreted bedrock geology of the southwest Yilgarn, *Geological Survey of Western Australia GSWA Record 2021/4*, 122-144 pp.

Salmon, M., B. L. N. Kennett, and E. Saygin (2013). Australian Seismological Reference Model (AuSREM): crustal component, *Geophys. J. Int.* **192,** 190-206, doi: 10.1093/gji/ggs004.

Salmon, M., S. Mousavi, and M. Sambridge (2022). 10 years of Australian Seismometers in Schools – education, outreach and research, *Australian Earthquake Engineering Society 2022 National Conference*, Mount Macedon, VIC.

Somerville, P., R. Graves, N. Collins, S.-G. Song, S. Ni, and P. Cummins (2009). Source and ground motion models for Australian earthquakes, *Australian Earthquake Engineering Society 2009 Conference*, Newcastle, New South Wales.

Waldhauser, F., and W. L. Ellsworth (2000). A double-difference earthquake location algorithm: Method and application to the Northern Hayward Fault, California, *Bull. Seismol. Soc. Am.* **90,** 1353–1368, doi: 10.1785/0120000006.

Yang, H., M. Quigley, and T. King (2021). Surface slip distributions and geometric complexity of intraplate reverse-faulting earthquakes, *Geol. Soc. Am. Bull.*, doi: 10.1130/B35809.1.

Zhang, M., W. L. Ellsworth, and G. C. Beroza (2019). Rapid earthquake association and location, *Seismol. Res. Lett.* **90,** 2276-2284, doi: 10.1785/0220190052.